

## Stress Analysis for Shrink fitting System used for Ceramics Conveying Rollers

HENDRA<sup>1,a</sup>, Masakazu TSUYUNARU<sup>1,b</sup>, Nao-Aki NODA<sup>1,c</sup>, Yasushi TAKASE<sup>1,d</sup>

<sup>1</sup>Department of Mechanical Engineering Kyushu Institute of Technology  
 Sensui-Cho 1-1 Tobata-Ku, Kitakyushu-Shi, Fukuoka, Japan

<sup>a</sup>mpe2\_boy@yahoo.com, <sup>b</sup>f344128m@tobata.isc.kyutech.ac.jp, <sup>c</sup>noda@mech.kyutech.ac.jp,  
<sup>d</sup>takase@mech.kyutech.ac.jp

**Keywords:** Finite element method, Elasticity, Bending and Maximum tensile stress.

**Abstract.** Cast iron and steel conveying rollers used in hot rolling mills must be changed very frequently because conveyed strips with high temperature induces wear on the roller surface in short periods. This failure automatically stops the production line for repair and maintenance of conveying rollers. In this study a new type of roller is considered where a ceramics sleeve is connected with two short shafts at both ends by shrink fitting. Here, a ceramics sleeve provides longer life and therefore reduces the cost for the maintenance. However, for the hollow ceramics rollers, care should be taken for maximum tensile stresses appearing at both edges of the sleeve. In particular, because fracture toughness is extremely smaller compared with the value of steel, stress analysis for the roller is necessary for ceramics sleeve. In this study FEM analysis is applied to the structure, and the maximum stress has been investigated with varying the dimensions of the structure. It is found that the maximum tensile stress appearing at the end of sleeves takes a minimum value at a certain amount of shrink fitting ratio.

### Introduction

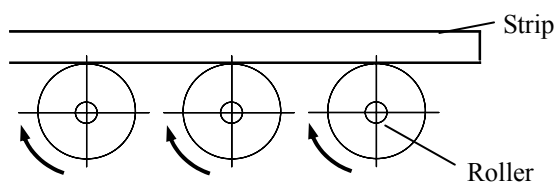


Fig.1 Layout of Conveying Rollers

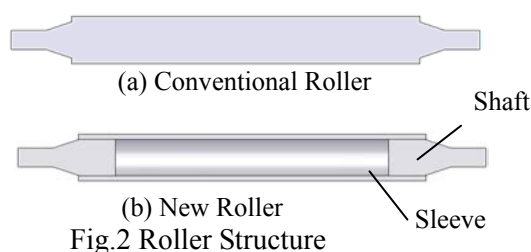


Fig.2 Roller Structure

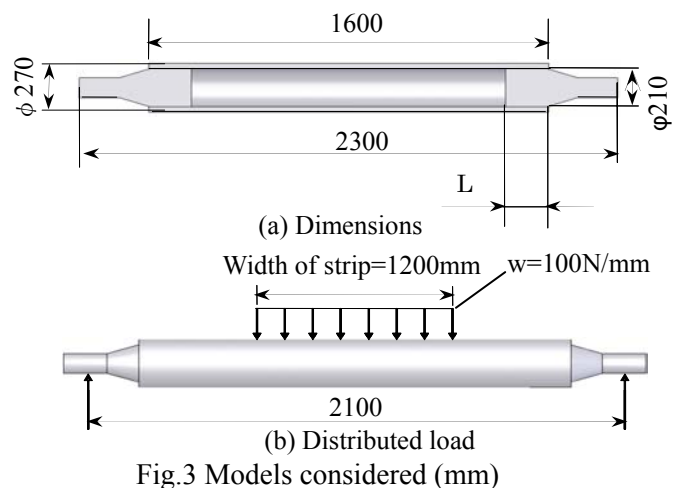


Fig.3 Models considered (mm)

Cast iron and steel conveying rollers used in hot rolling mills (see Fig.1) must be changed very frequently because conveyed strips with high temperature induces wear on the roller surface in short period. The damage portions have been repaired with the flame spray coating [1]. Use of ceramics and cemented carbide has been also promoted [2] because they have high temperature resistance and high abrasion resistance.

Figure 2(a) shows the structure of the conventional rollers. For conventional rollers material consumptions are large and the exchange cost of roller is high because we have to change whole

Table 1 Material Properties

	Young's modulus [GPa]	Poisson's ratio	Tensile strength [MPa]	Fracture toughness [MPa√m]
Ceramics	300	0.28	500	7.7
Cemented Carbide	500	0.24	1000	20
Steel	210	0.3	600	100

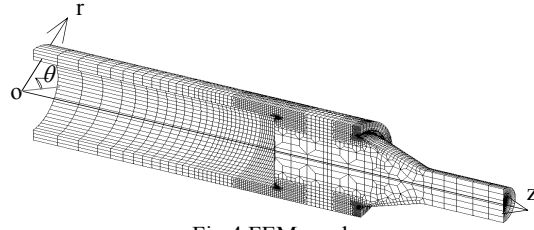
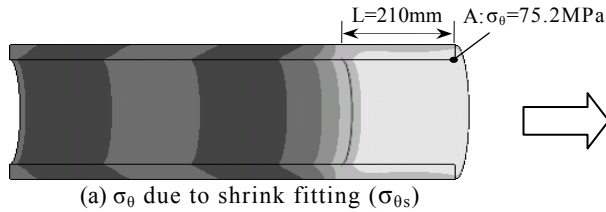
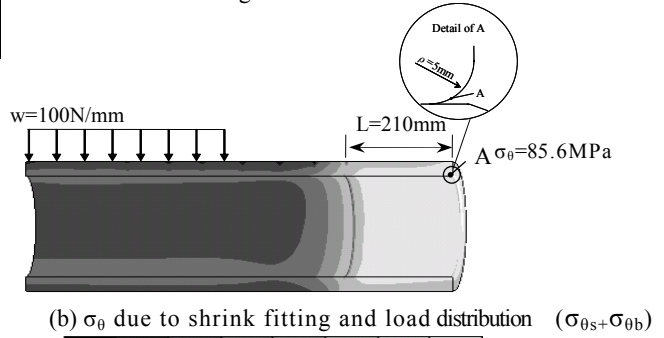


Fig.4 FEM mesh

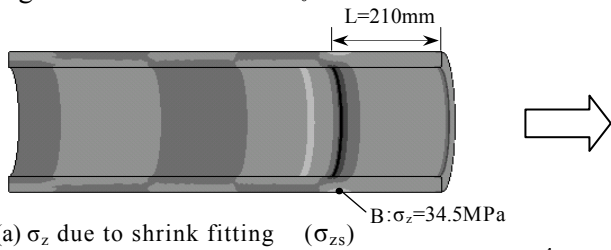


(a)  $\sigma_\theta$  due to shrink fitting ( $\sigma_{\theta s}$ )

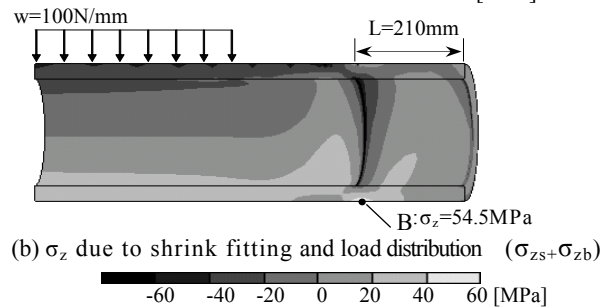


(b)  $\sigma_\theta$  due to shrink fitting and load distribution ( $\sigma_{\theta s} + \sigma_{\theta b}$ )

Fig.5 Stress distribution  $\sigma_\theta$  when  $\delta/d = 3.0 \times 10^{-4}$



(a)  $\sigma_z$  due to shrink fitting ( $\sigma_{z s}$ )



(b)  $\sigma_z$  due to shrink fitting and load distribution ( $\sigma_{z s} + \sigma_{z b}$ )

Fig.6 Stress distribution  $\sigma_z$  when  $\delta/d = 3.0 \times 10^{-4}$

roller. In this study, we will focus on the roller structure where a sleeve and two short shafts are connected by shrink fitting at both ends as shown in Fig.2 (b).

The new roller is suitable for maintenance and reducing the cost because we can exchange the sleeve only. In addition, the running speed of the steel strip can be changed smoothly due to the light weight. Moreover, further cost reduction can be realized if ceramics are used as the sleeve because they offer high temperature resistance and high abrasion resistance. However, for the hollow rollers, care should be taken for maximum tensile stresses appearing at the edge of the sleeve. Especially, because fracture toughness of ceramics is extremely smaller compared with the values of steel, stress analysis for the roller becomes important. Therefore, in this study FEM analysis is applied to the structure as shown in Fig.2 (b).

**Analytical Conditions**

Define the shrink fitting ratio as  $\delta/d$ , where  $\delta$  is the diameter difference with the diameter  $d=210\text{mm}$ . Assume that the roller is subject to distributed load  $w=100\text{N/mm}$  and simply supported at both ends (see Fig.3). The friction coefficient between sleeve and shafts is assumed as 0.3.

Table 1 shows the material properties of steel, ceramics and cemented carbide. Stainless steel is usually used for conventional rollers but ceramics and cemented carbide rollers may provide a longer maintenance span due to their high temperature resistance and high abrasion resistance.

Fig. 4 shows the finite element mesh model of the conveying rollers. The total number of elements is 22,340 and the total number of nodes is 26,751. The model of 1/4 of the roller is considered due to symmetry.

## Results and Discussion

### Maximum Tensile Stress

Figure 5 shows stress distribution  $\sigma_\theta$  at the shrink fitting ratio  $\delta/d = 3.0 \times 10^{-4}$ . Figure 5(a) shows the stress  $\sigma_{\theta_s}$  due to shrink fitting and Fig.5(b) shows maximum stress distribution  $\sigma_{\theta_{max}} (= \sigma_{\theta_s} + \sigma_{\theta_b})$  due to load distribution  $w=100\text{N/mm}$  after shrink fitting. As shown in Fig.5, the maximum tensile stress at point A is 75.2 MPa while shrink fitting. It becomes 85.6 MPa by applying the distribution load after shrink fitting, that is,  $\sigma_{\theta_b}=10.4$  MPa.

Figure 6 shows stress distribution  $\sigma_z$  at the shrink fitting ratio  $\delta/d = 3.0 \times 10^{-4}$ . Figure 6(a) shows the stress due to shrink fitting  $\sigma_{z_s}$  and Fig.6(b) shows maximum stress distribution  $\sigma_{z_{max}} (= \sigma_{z_s} + \sigma_{z_b})$  due to load distribution  $w=100\text{N/mm}$  after shrink fitting. As shown in Fig.6, the maximum tensile stress at point B is 34.5 MPa while shrink fitting. It becomes 54.5 MPa by applying the distribution

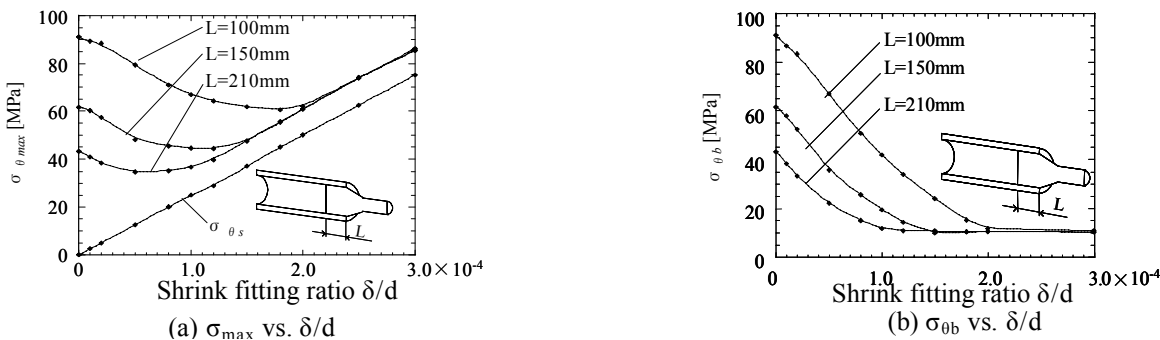


Fig.7  $\sigma_\theta$  vs.  $\delta/d$  when  $L=100, 150, 210\text{mm}$  ( $\sigma_{\theta_s}$ : Stress due to shrink fitting,  $\sigma_{\theta_b}$ : Stress due to load distribution)

load after shrink fitting, that is,  $\sigma_{z_b}=20.0$  MPa.

It is found understood that the maximum tensile stress appears at point A as  $\sigma_\theta$ . In this study we will focus on the maximum tensile stress  $\sigma_\theta$  at A with varying geometrical conditions.

### Effect of Shrink Fitting Ratio and Bending Moment upon the Maximum Tensile Stress $\sigma_{\theta_{max}}$

Figure 7 shows effects of Shrink Fitting Ratio and Bending Moment upon the Maximum Tensile Stress  $\sigma_{\theta_{max}}$ . Figure 7 (a) shows  $\sigma_{\theta_s}$  vs.  $\delta/d$  and  $\sigma_{\theta_{max}} (= \sigma_{\theta_s} + \sigma_{\theta_b})$  vs.  $\delta/d$  relations when the load distribution  $w=100\text{N/mm}$  is applied after shrink fitting. In Fig.7(b) shows  $\sigma_{\theta_b}$  vs.  $\delta/d$  relations when the load distribution  $w=100\text{N/mm}$  applied. When shrink fitting ratio  $\delta/d \geq 2.0 \times 10^{-4}$ ,  $\sigma_{\theta_b}$  becomes constant and independent of  $\delta/d$ . When  $\delta/d \geq 2.0 \times 10^{-4}$ , the shafts and sleeve can be treated as a unit body.

### The Effect of Fitted Length L on $\sigma_{\theta_{max}}$ and $\sigma_{\theta_b}$

If possible, small value of L is suitable for repairing and maintenance because the exchanges of the sleeve is easier for smaller L. Assume fitted length  $L=100\text{mm}, 150\text{mm}, 210\text{mm}$ . As shown in Fig.7 (a),  $\sigma_{\theta_s}$  is proportional to  $\delta/d$ , and independent of L. When the fitted length L becomes smaller,  $\sigma_{\theta_{max}}$  increases. From Fig.7 (a), it is found that  $\sigma_{\theta_{max}}$  has a minimum value 60.5MPa at  $\delta/d = 1.8 \times 10^{-4}$  when  $L=100\text{mm}$ . Similarly, it is found that the optimum shrink fitting ratio is  $\delta/d = 1.2 \times 10^{-4}$  when  $L=150\text{mm}$ , and also  $\delta/d = 5.0 \times 10^{-5}$  when  $L=210\text{mm}$ . When shrink fitting ratio  $\delta/d \geq 2.0 \times 10^{-4}$ ,  $\sigma_{\theta_b}$  becomes constant 10.5MPa independent of  $\delta/d$ .

### The Effect of Sleeve Materials on $\sigma_{\theta_{max}}$ and $\sigma_{\theta_b}$

Figure 8 shows  $\sigma_{\theta_{max}}$  vs.  $\delta/d$  and  $\sigma_{\theta_b}$  vs.  $\delta/d$  relations for different materials of conveying roller. As shown in Fig.8 (a), the maximum tensile stress of cemented carbide is larger than that of ceramics and steel because the Young's modulus  $E=500\text{MPa}$  is larger than the ones of ceramics and steel  $E=300\text{MPa}, E=210\text{MPa}$ .

### The Effect Radius Curvature $\rho$ on $\sigma_{\theta_{\max}}$ and $\sigma_{\theta_b}$

Figure 9 shows  $\sigma_{\theta_{\max}}$  vs.  $\delta/d$  and  $\sigma_{\theta_b}$  vs.  $\delta/d$  relations when the radius at the end of sleeve is changed as  $\rho=5, 10, 20, 30$ . From Fig.9(a), it is found that the maximum stress  $\sigma_{\theta_{\max}}$  increases with decreasing the radius  $\rho$ . The stress  $\sigma_{\theta_b}$  becomes constant at the same value of  $\delta/d$  independent of  $\rho$ .

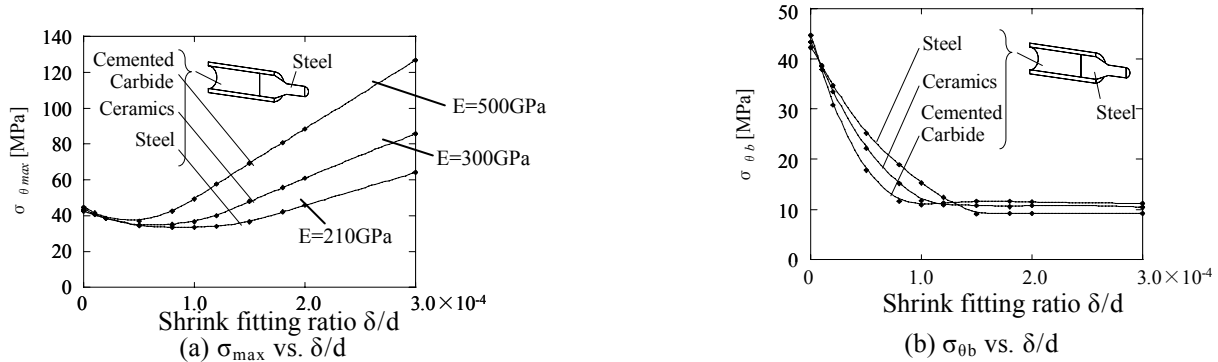


Fig.8  $\sigma_{\theta}$  vs  $\delta/d$  when Steel, Ceramics, Tungsten Carbide ( $\sigma_{\theta_{\max}} = \sigma_{\theta_s} + \sigma_{\theta_b}$ ,  $\sigma_{\theta_s}$ : Stress due to shrink fitting,  $\sigma_{\theta_b}$ : Stress due to load distribution)

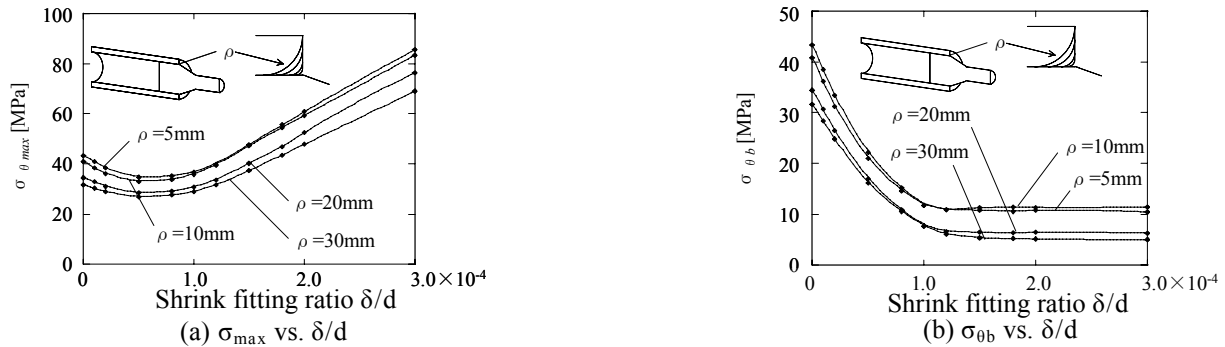


Fig. 9  $\sigma_{\theta}$  vs  $\delta/d$  when  $\rho=5, 10, 20, 30$  ( $\sigma_{\theta_{\max}} = \sigma_{\theta_s} + \sigma_{\theta_b}$ ,  $\sigma_{\theta_s}$ : Stress due to shrink fitting,  $\sigma_{\theta_b}$ : Stress due to load distribution)

### Conclusions

Conveyed strips with high temperature induce wear on the roller surface in short periods and maintenance cost increases by exchange the rollers. In this study, a ceramics sleeve connected with short steel shafts at both ends is considered. Stress analysis was performed with the application of the finite element method and the effects of fitted length  $L$ , sleeve materials, radius curvature  $\rho$  at the contact region were investigated. The conclusions can be made in the following way.

1. The value of maximum tensile stress is 85.6MPa when shrink fitting ratio  $\delta/d = 3.0 \times 10^{-4}$  and the load  $w=100\text{N/mm}$  distribution is applied after shrink fitting.
2. When shrink fitting ratio  $\delta/d \geq 2.0 \times 10^{-4}$ ,  $\sigma_{\theta_b}$  becomes constant and independent of  $\delta/d$ . When  $\delta/d \geq 2.0 \times 10^{-4}$ , the shafts and sleeve can be treated as a unit body.
3. The maximum stress  $\sigma_{\theta_{\max}}$  increases with decreasing the radius at the end of sleeve  $\rho$ . The stress  $\sigma_{\theta_b}$  becomes constant at the same value of  $\delta/d$  independent of  $\rho$ .

### References

- [1] Miki, E., "High Corrosion Resistance and Cost Reduction by Spraying Methods", *Plant Engineer*, Vol.21, No.1 (1989), pp.8-12 (in Japanese).
- [2] Iwata, T. and Mori, H., "Material Choice for Hot Run Table Roller", *Plant Engineer*, Vol.15, No.6 (1983), pp.55-59 (in Japanese).
- [3] S. Harada, N. Noda, O. Uehara and M. Nagano, "Tensile strength of hot isostatic pressed silicon nitride and effect of specimen dimension", *Journal of the Japan society of mechanical engineering*, Vol.57, No.539 (1991).
- [4] H. Kobayashi and T. Kawakubo, "Fatigue -Difference between ceramics and metal-", *Journal of the Japan institute of metals*, Vol.27, No.10 (1988).
- [5] Editorial Committee of Ceramic Society of Japan, "Material properties of ceramics", pp.34-36 (1979), Ceramic Society of Japan.

---

**Advances in Fracture and Damage Mechanics VII**

doi:10.4028/www.scientific.net/KEM.385-387

**Stress Analysis for Shrink Fitting System Used for Ceramics Conveying Rollers**

doi:10.4028/www.scientific.net/KEM.385-387.513